



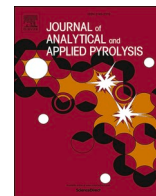
## **Comparing bed materials for fluidized bed steam cracking of high-density polyethylene: Olivine, bauxite, silica-sand, and feldspar**

Downloaded from: <https://research.chalmers.se>, 2025-12-10 01:14 UTC

Citation for the original published paper (version of record):

Mandviwala, C., González Arias, J., Berdugo Vilches, T. et al (2023). Comparing bed materials for fluidized bed steam cracking of high-density polyethylene: Olivine, bauxite, silica-sand, and feldspar. *Journal of Analytical and Applied Pyrolysis*, 173. <http://dx.doi.org/10.1016/j.jaap.2023.106049>

N.B. When citing this work, cite the original published paper.



# Comparing bed materials for fluidized bed steam cracking of high-density polyethylene: Olivine, bauxite, silica-sand, and feldspar

Chahat Mandviwala<sup>\*</sup>, Judith González-Arias, Teresa Berdugo Vilches, Martin Seemann, Henrik Thunman

Department of Space, Earth and Environment (SEE), Division of Energy Technology, Chalmers University of Technology, Gothenburg 412 96, Sweden

## ARTICLE INFO

### Keywords:

Steam cracking  
Fluidized bed  
Petrochemicals  
Plastic waste  
Polyethylene  
Natural ores

## ABSTRACT

Steam cracking in fluidized beds is an alternative method for producing valuable petrochemicals from plastic waste. Previous studies on the conversion of plastics in fluidized beds have revolved around non-catalytic cracking using silica sand as the bed material. On the other hand, studies on catalytic cracking have focused on the use of active materials such as olivine, bauxite, feldspar, and zeolites. The potential influence of the above-mentioned materials, in their natural or inactive state, on fluidized bed hydrocarbon cracking, is not well-documented in the literature. In this paper, steam cracking of polyethylene in a bubbling fluidized bed at 750 °C is investigated in the presence of four different natural ores: olivine, bauxite, silica sand, and feldspar. The paper compares the performance of the steam cracking process in terms of cracking severity, conversion, and product distribution among different hydrocarbon groups. The results show that there is only a marginal difference in cracking severity among the different bed materials, while the conversion remain relatively consistent, ranging from 93% to 95% (carbon.%). The yields of paraffins and carbon oxides are narrow, ranging from 15% to 16% and 3–4%, respectively, while the yields of light olefins and aromatics show a slightly wider range. The yield of olefins is in the range of 52–57%, and for aromatics, it ranges from 16% to 21%. The paper also discusses the potential impact of these bed materials on the cracking reactions, including their thermal and reactive interactions.

## 1. Introduction

The production of petrochemicals, including olefins, aromatics, synthesis gas, and methane, is essential for many modern products, such as plastics, clothing, medical equipment, and automobiles. These petrochemicals are primarily derived from steam cracking of petroleum-based resources, which poses significant sustainability challenges. In a scenario where the use of fossil resources is phased out, a paradigm shift is necessary regarding the production of petrochemicals. Within this framework, an alternative approach would be to use waste streams that are rich in plastic materials through steam cracking as a way to produce petrochemicals. This method has the potential to address sustainability challenges in petrochemical production by utilizing readily available waste streams that are rich in plastic and leveraging the similarities between the molecular structures of common fossil feedstocks and specific plastic materials like polyolefins [1–3].

Plastic production has increased substantially in recent decades,

resulting in a significant amount of plastic waste that is contaminating the environment. If current plastic production and waste management practices persist, it is projected that by 2050, the world will have amassed 12 billion tons of plastic waste in natural habitats or landfills. Of particular concern are polyolefins, which account for approximately 65% of the current plastic production capacity [4]. Polyolefins are long-chained saturated hydrocarbons similar to petroleum naphtha, and therefore waste streams that contain high concentrations of polyolefins can be utilized as a feedstock for the steam cracking process to meet the surging demand for petrochemicals [1,5].

As of today, steam cracking is performed in tubular flow reactors inside a furnace where hydrocarbons are cracked, and the furnace provides the necessary heat for the cracking reactions [6]. However, waste streams rich in polyolefins, which have been proposed as an alternative feedstock for steam cracking, are more complex than traditional petroleum-based feedstocks. These waste streams, due to their complex composition consisting of a heterogeneous mixture of plastic, biogenic,

<sup>\*</sup> Corresponding author.

E-mail address: [chahat@chalmers.se](mailto:chahat@chalmers.se) (C. Mandviwala).

<https://doi.org/10.1016/j.jaap.2023.106049>

Received 12 April 2023; Received in revised form 27 May 2023; Accepted 7 June 2023

Available online 9 June 2023

0165-2370/© 2023 The Authors. Published by Elsevier B.V. This is an open access article under the CC BY license (<http://creativecommons.org/licenses/by/4.0/>).

and inorganic wastes, are not suitable for processing in traditional tubular steam crackers [3].

Several studies have investigated the conversion of plastics to light olefins (C2–C4) under process conditions similar to those of a typical steam cracking process, using various reactor configurations. Milne et al. used an internally circulating fluidized bed reactor to convert low-density polyethylene (LDPE) to light olefins, achieving a maximum yield of 65% at a cracking temperature of 805 °C [7]. Artetxe et al. investigated the conversion of polyethylene to light olefins in a two-step process, with the first stage being a conical spouted bed reactor operated at 500 °C, and the second stage being a tubular reactor operated in the range of 800–950 °C [8]. The study obtained a yield of 77 wt% of light olefins at 900 °C in the second step. More recently, Fu et al. also used a two-stage tubular reactor to study the evolution of light olefins from the pyrolysis of polyethylene, achieving a maximum yield of 76 wt% at 800 °C in the second stage [9]. These studies indicate that the conversion of polyethylene at temperatures around 800 °C is a promising approach for the production of light olefins. Additionally, fluidized bed reactors are a suitable option for converting plastic waste to light olefins.

Fluidized bed reactors are considered suitable for steam cracking of highly heterogeneous feedstocks, such as plastic waste, because of their heat transfer and mixing properties [1,2]. These properties of a fluidized bed reactor are exclusively attributed to the presence of a solid bed material inside the reactor [1,2]. Moreover, the bed material can also serve as catalytically active sites to promote the cracking reactions [10]. Therefore, an appropriate choice of bed material becomes a key parameter in the successful implementation of such a fluidized bed steam cracking process.

The bed material used in a fluidized bed steam cracker must be capable of withstanding the severe mechanical conditions that arise during fluidization [11]. Additionally, the bed material should be resistant to the exposure of ash and noxious gases involving sulfur, chlorine, or phosphorus that may originate from plastic waste. A certain level of bed material replacement becomes unavoidable when the bed material used is susceptible to the above-mentioned conditions, which means that inexpensive materials, such as natural ores, are preferable [11]. In addition to the physical properties, the chemical composition of the bed material is also crucial. The presence of hazardous species, such as nickel, would prevent the used bed material from being disposed of into the environment without any pretreatment. More importantly, the chemical species present in the bed material should remain inert towards the produced hydrocarbon products to avoid undesirable secondary reactions. For instance, the transition metal oxide content of the bed material is synonymous with a propensity to oxidize a certain amount of the feedstock in the fluidized bed, which leads to a lower formation of valuable hydrocarbons such as ethylene and propylene [12].

The performance of the cracking process is influenced by the choice of bed material due to two types of interactions that can occur between the bed material and the cracking reactions: thermal interactions and reactive interactions [13]. Thermal interactions influence the cracking severity, which determines the degree to which the hydrocarbon feedstock is broken down into smaller molecules [13]. On the other hand, reactive interactions are associated with the catalytic activity of the bed material towards steam cracking reactions, potentially altering the product distribution or reaction pathways [13]. A thorough understanding of these interactions is essential for selecting the optimal bed material to achieve the desired cracking performance.

Research conducted over three decades on fluidized bed steam cracking of plastics has, to a great extent, revolved around the use of natural ores such as silica-sand, bauxite, and olivine as bed materials mainly because of their low cost and resistance to the harsh process conditions [1,2]. Additionally, several researchers have utilized feldspar as a bed material in fluidized bed conversion processes, considering the previously discussed criteria for a suitable bed material [11,14]. Of the four natural ores mentioned above, silica-sand has been the most widely

explored bed material for steam cracking of plastic materials in fluidized beds. Silica sand, being composed primarily of SiO<sub>2</sub> (> 90 wt%), is typically considered chemically inert towards the cracking reactions [2, 11,15]. Due to this characteristic, it is often used as a reference bed material for experimental research to evaluate the catalytic effects of other bed materials. In contrast, bauxite, olivine, and feldspar have been proven to exhibit catalytic activity in a hydrocarbon-steam environment within fluidized beds.

A recent study revealed that bauxite can play a role in promoting hydrocracking reactions during fluidized bed steam cracking, thereby increasing the hydrogen-to-carbon ratio of the products [13]. Some researchers have utilized olivine, activated with biomass ash, which has the ability to catalyze steam reforming reactions, to increase the production of syngas during steam cracking [5,16]. Similarly, feldspar has also been demonstrated to catalyze the steam reforming reactions of hydrocarbons in fluidized beds [11,17]. Given that feldspar is an aluminosilicate, it may possess catalytic properties similar to zeolites, which are the most widely used fluid catalytic cracking (FCC) catalysts. However, to the authors' knowledge, there have been no previous studies investigating the use of feldspar as the bed material in a fluidized bed hydrocarbon cracker.

The catalytic activities of bauxite, olivine, and feldspar in fluidized beds have been reported to arise from either chemical modification of the bed material or the addition of external species to the bed material [5,11,13,17]. For example, bauxite was demonstrated to promote hydrocracking exclusively in a reduced oxidation state, while olivine and feldspar displayed catalytic properties after the bed material surface was exposed to biomass ash. The potential influence of these bed materials in their natural state is largely unknown, despite their critical importance. To address this gap in knowledge, a systematic comparison is necessary to evaluate the potential influences of these bed materials in their natural state on the steam cracking of hydrocarbons. Such a study can provide valuable insights into the optimal selection of bed materials for fluidized bed steam cracking processes.

The aim of this paper is to compare the performance of olivine, bauxite, silica-sand, and feldspar as bed materials in a bubbling fluidized bed (BFB) steam cracker. High-density polyethylene (HDPE) was used as the feedstock for the steam cracker. HDPE was used in its virgin form to minimize the potential influences of feedstock impurities on the cracking reactions, and the bed materials. The performance of the steam cracker was analyzed in terms of the conversion, cracking severity, and the yields of valuable hydrocarbons such as light olefins and monoaromatics. The thermal and reactive interactions of the bed materials were also compared. Elemental carbon and hydrogen balances over the steam cracker were calculated and used as a tool to analyze the performance parameters.

## 2. Fundamentals and definitions

The performance of a steam cracking process is measured through cracking severity, a commonly used parameter in the petrochemical industry. Additionally, the conversion and the distribution of products among hydrocarbon groups, such as olefins and aromatics, is also taken into consideration as means of comparing the performance of the steam cracker. The performance parameters can be comprehended using the mass balance over the steam cracker.

### 2.1. Carbon and hydrogen balance

The determination of carbon and hydrogen balances in a steam cracking process is crucial because the feedstock typically consists of a pure hydrocarbon stream composed primarily of carbon and hydrogen atoms.

In this work, the carbon balance is calculated by summing the contribution of all carbon-containing species in the product mixture. Similarly, the hydrogen balance is calculated by summing the contri-

bution of all hydrogen-containing species in the product mixture. The contribution of species  $i$  to the carbon and hydrogen balance is calculated according to Eqs. 1 and 2, respectively.

$$\%C_i = \frac{n_i}{nC_T} \times c_i \times 100 \quad (1)$$

$$\%H_i = \frac{n_i}{nH_T} \times h_i \times 100 \quad (2)$$

Here,  $n_i$  represents the yield of species  $i$  in mol/kg.  $nC_T$  and  $nH_T$  represents the total moles of carbon and hydrogen present in 1 kg of feedstock, respectively.  $c_i$  and  $h_i$  represents the number of carbon and hydrogen atoms present in one molecule of species  $i$ , respectively.

In analyzing the hydrogen balance, it is important to consider the origin of hydrogen (as  $H_2$ ), which can be attributed to two sources: the feedstock and reacted water through steam reforming or water gas shift reactions. However, for the calculation of hydrogen balance, as shown in Eq. 2, only the amount of hydrogen present in the plastic feedstock is considered. It is important to subtract the amount of hydrogen originating from steam reforming and water gas shift reactions from the total yield of hydrogen (as  $H_2$ ). This is done to obtain a clear and precise calculation of the amount of hydrogen originating solely from the plastic feedstock. The amount of  $H_2$  originating from the plastic feedstock is calculated according to Eq. 3.

$$n_{H_2} = n_{H_2(\text{total})} - n_{CO} - 2 \times n_{CO_2} \quad (3)$$

Eq. 3 is based on the stoichiometric steam reforming and water gas shift reactions. Eq. 3 is applicable only when the feedstock used for steam cracking does not contain oxygen.

## 2.2. Conversion

In the petrochemical industry, the conversion rate in a typical steam cracker refers to the percentage of feedstock that is successfully broken down into smaller molecules through the cracking process [6,18]. The conversion rate, in this work, is quantified as the total yield of C1-C4 species, aromatic, polycyclic aromatic hydrocarbons (PAHs) and carbon deposits. Aliphatic hydrocarbons with chain lengths of C5 and above are not included in conversion rate due to limitations in the scope of the analytical equipment used. This allowed an accurate assessment of the steam cracking process in terms of converting the feedstock, while acknowledging the limitations of our analytical methods. Furthermore, these species are generally considered unconverted in the industrial steam cracking process, as their conversion typically requires a secondary cracking step downstream, such as FCC or hydrocracking [6]. Aromatic and PAHs are included when calculating the conversion since these hydrocarbons are essentially produced from cracking of linear hydrocarbons and do not require a secondary cracking step. The calculation of conversion is given by Eq. 4.

$$\text{conversion rate} = \%C_{CO_x} + \%C_{CH_4} + \%C_{C_2H_6} + \%C_{C_3H_8} + \%C_{C_4H_{10}} + \%C_{\text{aromatics}} + \%C_{\text{PAHs}} + \%C_{\text{carbon deposits}} \quad (4)$$

Here,  $\%C_i$  is calculated using Eq. 1.

## 2.3. Cracking severity

Cracking severity is a parameter used in the operation of steam crackers, to describe the extent to which hydrocarbons are broken down or 'cracked' into smaller molecules [6]. This work proposes a cracking severity coefficient that represents the amount of light olefins ( $C_2H_4$ ,  $C_3H_6$ , and  $C_4H_8$ ) generated per molecule of methane produced. A higher cracking severity coefficient corresponds to lower cracking severity. The cracking severity coefficient is a comparative parameter and can be used to compare the performance of two or more steam cracking operations. The calculation of the cracking severity coefficient is given by Eq. 5.

$$\text{cracking severity coefficient} = \frac{n_{C_2H_4} + n_{C_3H_6} + n_{C_4H_8}}{n_{CH_4}} \quad (5)$$

The parameters mentioned above are used to compare the experimental cases presented in the paper, and they adhere to the experimental procedure described in the following section.

## 3. Materials and method

### 3.1. Materials

The bed materials investigated in this work were bauxite, olivine, silica-sand and feldspar. The physical and fluidization properties of the bed materials, including the particle density, mean particle size, and minimum fluidization velocity, are summarized in Table 1. The chemical compositions of the bed materials, as described by the suppliers, are detailed in Table 2.

HDPE pellets, used as the feedstock for the investigation described in this work, were provided by Borealis AB (Stenungsund, Sweden). The HDPE pellets had a bulk density of 945 kg/m<sup>3</sup> and an average pellet size of 2.5 mm. The proximate analysis and the chemical composition of the HDPE pellets is summarized in Table 3.

### 3.2. Experimental setup

The experimental setup used in this work is shown in Fig. 1. The steam cracking tests were performed in a laboratory-scale BFB reactor. The BFB reactor, used in this work, is constructed of stainless steel, with an internal diameter of 88.9 mm and a height of 1305 mm. The reactor is placed inside an electrically heated oven. To monitor the temperature during the experiments, three thermocouples are placed within the reactor. One of these thermocouples is submerged in the fluidized bed, while the other two are located in the freeboard. The temperature in the freeboard region is regulated to match that of the bed material. The bed materials are loaded from the top of the reactor before heating the reactor. After each set of experiment, the reactor is cooled down and cleaned with a vacuum cleaner before loading a different batch of bed material.

The gases used to fluidize the bed are introduced from the bottom of the reactor and can be changed between nitrogen, air, helium, steam, or a combination of these. The fluidization gases are mixed homogeneously in a mixer before entering the reactor. The steam is produced in an evaporator equipped with a liquid flow controller (LFC). The helium, nitrogen and air are supplied by mass flow controllers (MFC). Nitrogen flow (2 L<sub>m</sub>/min) is provided to maintain a stable steam flow and prevent back-mixing of atmospheric air from the top of the reactor. A small flow of helium (0.05 L<sub>m</sub>/min) is used as a tracer gas for quantification of the total dry gas flow from the reactor.

Two parallel slipstreams of gas (S1 and S2) are sampled from the probe inserted into the reactor, as shown in Fig. 1. The gas sampling probe is maintained at 350 °C with an electrical heating band, to avoid condensation of steam and hydrocarbons. The measurement techniques applied to each splitstream, along with the parameters quantified through each measurement, are summarized in Table 4.

Slipstream 1 is used for sampling condensable hydrocarbons and

**Table 1**

Physical properties and estimated minimum fluidization velocity of the tested bed materials.

	Olivine	Bauxite	Silica-sand	Feldspar
Particle density (kg/m <sup>3</sup> )	3300	3000	2650	2600
Mean particle diameter, $d_p$ (μm)	288	305	316	200
Minimum fluidization velocity, $u_{mf}$ (m/s)	0.05	0.05	0.04	0.03

**Table 2**  
Chemical composition (%wt.) of the tested bed materials.

	Olivine	Bauxite	Silica-sand	Feldspar
SiO <sub>2</sub>	41.7	6.5	90	67.5
Al <sub>2</sub> O <sub>3</sub>	0.17	88.5	5.5	18.8
Fe <sub>2</sub> O <sub>3</sub>	7.4	1.1	0.6	0.11
TiO <sub>2</sub>	-	3.0	-	0.01
MgO	49.6	-	-	0.04
Na <sub>2</sub> O	-	-	1.2	4.3
K <sub>2</sub> O	-	-	1.8	8.4

**Table 3**  
Properties of the HDPE pellets used in this work.

Proximate analysis	%wt.
Moisture content	0.00
Volatile matter	99.92
Fixed carbon	0.00
Ash content	0.08
<b>Chemical composition %wt.</b>	
Carbon	85.70
Hydrogen	14.20

permanent gases produced from the steam cracking of HDPE. The condensable hydrocarbons are measured using the SPA method as described by Israelsson et al. [19]. The method proposed by Israelsson et al. involves sampling the product gas through one double-layered adsorption column with amino propyl-bonded and activated carbon layers [19]. In this work, a series of two double-layered adsorption columns is used to ensure complete adsorption of the condensable hydrocarbons present in the product gas. The SPA tubes used in this work are Supelclean ENVI-Carb/NH<sub>2</sub> tubes obtained from Sigma-Aldrich. The condensable hydrocarbons adsorbed on the SPA tubes are quantified with a BRUKER GC-FID system. The GC-FID quantifiable species are exclusively aromatic hydrocarbons, including benzene, toluene, xylenes, styrene, naphthalene and its derivatives, and some other polycyclic aromatic hydrocarbons (PAHs). A comprehensive list of the GC-FID quantifiable species is provided by Israelsson. et. al [19]. The detection and

quantification of aliphatic and naphthenic hydrocarbons present in the condensable are out of the scope of the SPA method.

The non-condensable gases leaving the SPA tubes are collected in 0.5-liter Tedlar gas bags. The volumetric composition (%vol) of the sampled gas bags is measured using an Agilent 490 micro-GC system equipped with PoraPLOT U, CP-COX, and CP-Sil 5 CB columns and a thermal conductivity detector (TCD) for each column. The micro-GC system is calibrated for quantifying He, H<sub>2</sub>, CO, CO<sub>2</sub>, Air (O<sub>2</sub> + N<sub>2</sub>), CH<sub>4</sub>, C<sub>2</sub>H<sub>4</sub>, C<sub>2</sub>H<sub>6</sub>, C<sub>3</sub>H<sub>8</sub>, and C<sub>4</sub>H<sub>10</sub>. The quantification of individual C<sub>3</sub> and C<sub>4</sub> hydrocarbons is not possible due to coelution and are therefore lumped together as C<sub>3</sub>H<sub>8</sub> and C<sub>4</sub>H<sub>10</sub>, respectively.

Slipstream 2 is used for continuous monitoring of permanent gases including, H<sub>2</sub>, O<sub>2</sub>, CO, CO<sub>2</sub>, and CH<sub>4</sub>, in the product gas. The continuous measurement is performed using a SICK GMS 820 permanent gas analyzer (manufactured by SICK AG). The product gas is dried and

**Table 4**  
Measurement techniques applied to sampled slipstreams.

	Measurement method	Technical description
Slipstream 1	Solid-phase adsorption (SPA)	SPA tubes: A series of 2 interconnected SPA tubes, each consisting of a double adsorbent layer of amino propyl-bonded silica and activated carbon. Analytical instrument: BRUKER GC-430 equipped with flame ionization detector (GC-FID). Species quantified: from Benzene to Triphenylene.
	Permanent gas analysis	Gas bags: 0.5-L Tedlar® gas bags connected downstream of the SPA tubes. Analytical Instrument: Agilent 490 micro-GC system equipped with PoraPLOT U, CP-COX and CP-Sil 5 columns. Species quantified: He, H <sub>2</sub> , CO, CO <sub>2</sub> , Air (coelution of O <sub>2</sub> and N <sub>2</sub> ), CH <sub>4</sub> , C <sub>2</sub> H <sub>4</sub> , C <sub>2</sub> H <sub>6</sub> , C <sub>3</sub> H <sub>8</sub> , and C <sub>4</sub> H <sub>10</sub> .
Slipstream 2	Continuous gas analysis	Analytical instrument: SICK GMS 820 permanent gas analyzer (SICK AG, Waldkirch, Germany). Species quantified: H <sub>2</sub> , O <sub>2</sub> , CO, CO <sub>2</sub> , and CH <sub>4</sub> .

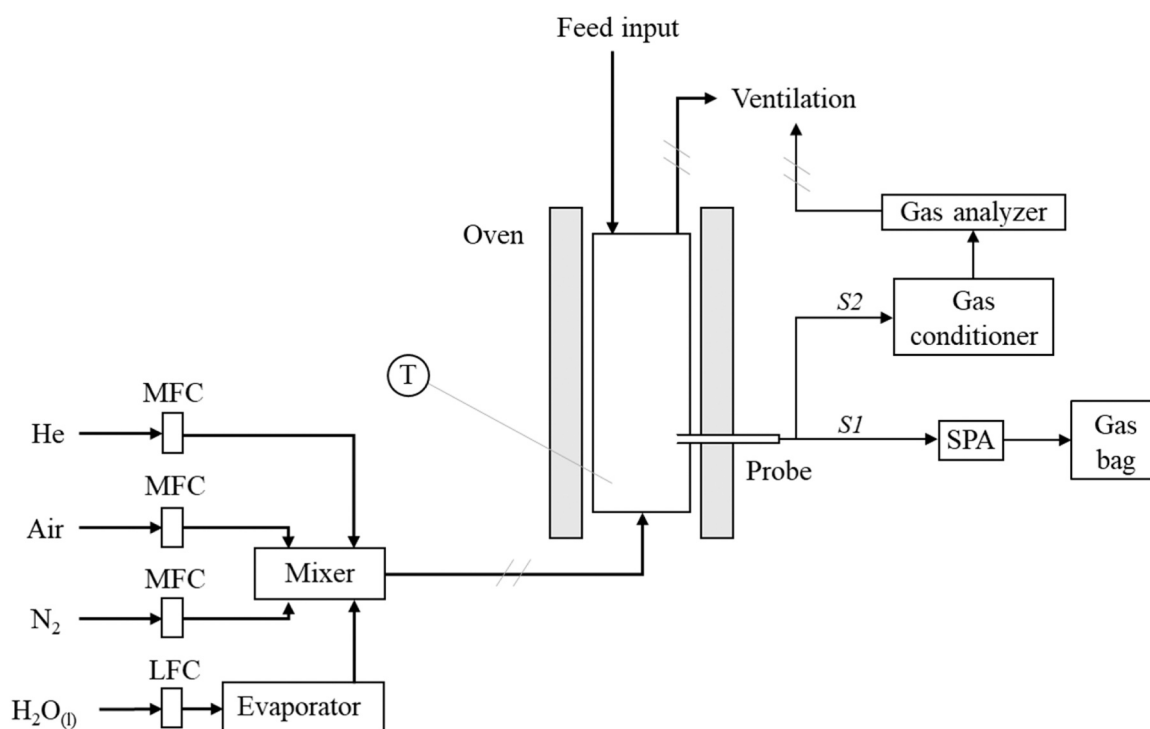


**Fig. 1.** Schematic of the experimental setup applied for the steam cracking experiments.



cooled by scrubbing it with isopropanol in a gas conditioning system before it is acquired by the permanent gas analyzer. Continuous measurement of the product gas is performed to determine the total reaction time and ensure that there is no leakage of atmospheric oxygen into the reactor system during the experiments.

### 3.3. Steam cracking tests

The steam cracking experiments were conducted in batch mode at a bed material temperature of 750 °C. Several studies have reported an optimal cracking temperature range of 750–850 °C for the production of light olefins from polyethylene [7–9,15,20]. In our study, a cracking temperature of 750 °C was selected to investigate the influence of bed materials on the production of light olefins. The aim of the study was not to determine the optimal temperature for cracking but rather to evaluate the performance of different natural ores as bed materials at a temperature that is known to promote the production of light olefins.

In each batch, 2 g of HDPE pellets were directly fed onto the top of the hot fluidized bed. A high bed material to feed ratio of 250 (500 g bed material) was employed to prevent defluidization within the reactor. At least four batch experiments were conducted for each bed material, and the results presented are the average values of these four repetitions. Each set of experiments were performed systematically in three stages. The procedure for each set of the experiments along with the reaction conditions during each of the three stages are summarized in Table 5.

Following Table 5, the fluidization gases were cycled through the three stages of the experimental procedure. Stage one involved the inertization of the reactor through fluidization with nitrogen before the feeding of HDPE pellets. The reactor was considered inert when the O<sub>2</sub> concentration measured by the SICK permanent gas analyzer was recorded as 0% vol in the gases leaving the reactor. During stage two, the reactor was supplied with steam while a batch of HDPE pellets was fed simultaneously. The reaction time for steam cracking was determined to be approximately 45 s based on readings from the permanent gas analyzer. Subsequently, gases produced during this stage were collected and analyzed over a 120-second interval using the two slipstreams. This ensured that the products were sampled throughout the entire conversion time, allowing for a comprehensive analysis of the gas composition. In the final stage, the carbon deposits on the bed material were oxidized to CO and CO<sub>2</sub> through fluidization with air. Carbon oxides released during this stage were quantified with the micro-GC system to determine the total yield of carbon deposits on the bed material. Complete oxidation was indicated when the O<sub>2</sub> concentration in the effluent gases matched the ambient O<sub>2</sub> concentration of 20.9% vol.

In each experiment, a specified volume of helium (He) was used as one of the fluidization gases during both the steam cracking and combustion stages. The inclusion of a known volume of He in the fluidization mixture enabled the calculation of the total volume of gases generated during these stages. Throughout the experiment, the fluidization gas flow rate was maintained at a value corresponding to a fluidization velocity that was 10–12 times the minimum fluidization velocity ( $u_{mf}$ ) of the employed bed materials.

### 3.4. Data evaluation

The results reported in the subsequent sections represent the average values obtained from the four repetitions of each experiment. The results

**Table 5**  
Experimental procedure for the steam cracking tests.

Experimental stage	Fluidization gases (l <sub>N</sub> /min)				Time
	Nitrogen	Steam	Air	Helium	
1. Inertization	2.0	0.0	0.0	0.00	Until 0%vol O <sub>2</sub>
2. Steam cracking	2.0	4.0	0.0	0.05	120 s
3. Combustion	0.0	0.0	5.0	0.05	Until 20.9%vol O <sub>2</sub>

were obtained through consistent sampling, analysis, and evaluation procedures, thereby ensuring that the identified trends surpass the systematic errors for all data points.

The molar yields (mol/kg<sub>HDPE</sub>) of the gaseous species collected in the Tedlar gas bags were determined using the He-tracing method. The calculation of the molar yields of the measured gaseous species was performed using Eq. (6), which is expressed as:

$$n_i = \frac{c_i}{m_{HDPE}} \times \left( \frac{V_{He-tracing}}{C_{He}} \right) \times \frac{1}{V_m} \quad (6)$$

Here,  $n_i$  represents the molar yield,  $c_i$  represents the concentration (%vol.) of the gaseous species  $i$ ,  $C_{He}$  and  $V_{He-tracing}$  represent the concentration and volume of the tracer gas, respectively,  $m_{HDPE}$  denotes the weight of the HDPE pellets for each batch, and  $V_m$  represents the volume of one mole of an ideal gas at 0 °C. Subsequently, the molar yield of each species was transformed into the corresponding carbon and hydrogen yields (%carbon and %hydrogen) based on the carbon and hydrogen composition of the feedstock (as detailed in Table 3).

## 4. Results

The results obtained in this work are presented in the form of carbon and hydrogen balance, conversion, and the cracking severity, in the following sections.

### 4.1. Carbon balance

Table 6 presents the complete carbon balance for the experiments conducted with the four bed materials. The yields of individual species are reported in terms of their contribution to the carbon balance (% carbon). Reporting the yields in the form of carbon balance provides a clearer understanding of the product distribution, as the feedstock primarily consists of carbon and hydrogen (see Table 3). It is worth noting that closing the balance using yields calculated based on the weight of the feedstock can be ambiguous, specifically for carbon oxides, as the oxygen can be derived from water molecules present in the reaction mixture. Therefore, carbon-based yields are provided to close the carbon balance, while mass-based yields (in parentheses) are provided for a fair

**Table 6**  
Elemental carbon balance over the steam cracker. The yields are reported in terms of the contribution (%carbon) of each species to the carbon balance. The percentage yields provided in parentheses correspond to the yields calculated based on the mass balance of the feedstock (%wt. feedstock).

	Olivine	Bauxite	Silica-sand	Feldspar
%carbon. (%wt. feedstock)				
C <sub>2</sub> H <sub>4</sub>	31.19 (31.18)	29.47 (29.46)	28.29 (28.28)	31.75 (31.74)
C <sub>3</sub> H <sub>x</sub>	16.86 (16.85)	14.71 (14.70)	14.26 (14.25)	16.59 (16.58)
C <sub>4</sub> H <sub>x</sub>	8.63 (8.33)	8.27 (7.99)	10.37 (10.01)	9.04 (8.73)
CH <sub>4</sub>	10.93 (12.49)	11.09 (12.67)	11.13 (12.71)	11.11 (12.69)
C <sub>2</sub> H <sub>6</sub>	4.31 (4.62)	3.86 (4.13)	5.29 (5.67)	3.96 (4.24)
Benzene	9.39 (8.73)	8.97 (8.34)	8.24 (7.66)	8.33 (7.74)
Toluene	3.39 (3.19)	3.59 (3.37)	4.22 (3.97)	3.53 (3.32)
Xylene	0.51 (0.48)	0.51 (0.48)	0.59 (0.56)	0.29 (0.27)
Styrene	1.53 (1.42)	1.62 (1.51)	1.92 (1.78)	1.09 (1.01)
Naphthalene	1.47 (1.35)	1.65 (1.51)	2.22 (2.03)	1.27 (1.16)
Others	2.63 (2.41)	4.35 (3.98)	3.29 (3.01)	1.83 (1.67)
CO	0.79 (1.58)	1.01 (2.02)	1.31 (2.62)	0.78 (1.56)
CO <sub>2</sub>	2.25 (7.07)	2.56 (8.04)	3.04 (9.55)	2.54 (7.98)
Carbon deposits	1.04 (0.89)	1.54 (1.32)	1.06 (0.91)	1.48 (1.27)
Balance <sup>a</sup>	5.05 (n.d. <sup>b</sup> )	6.81 (n.d.)	4.79 (n.d.)	6.41 (n.d.)

<sup>a</sup> 'Balance' represents the difference between the total carbon in the feedstock and the amount of carbon in the measured products.

<sup>b</sup> n.d.: not determined.

comparison of the obtained results with the existing literature.

The results showed that the carbon balance closure values for the four bed materials were 95%, 93%, 95%, and 94% for olivine, bauxite, silica-sand, and feldspar, respectively. The total yield of light hydrocarbon species ( $C_1$ ,  $C_2$  and  $C_3$ ), on the basis of carbon balance, ranges from 67.4% to 72.4% among the four bed materials, with feldspar yielding the highest percentage.  $C_2H_4$  is the dominant species for all the bed materials, accounting for approximately 1/3rd of the product distribution.  $C_3H_x$  and  $C_4H_x$  species are also present in significant amounts, with feldspar giving the highest percentage of both.

The total aromatics yield, based on the carbon balance, ranges from 16.34% to 20.69% among the four bed materials, with bauxite having the highest percentage. Benzene is the dominant aromatic compound for all four bed materials, followed by toluene, xylene, styrene, and naphthalene. The proportion of each of these aromatic compounds varies slightly among the bed materials.

The other product groups, namely paraffins, carbon oxides, and carbon deposits, had smaller contributions to the carbon balance, with paraffins contributing 14.96–16.42%, total carbon oxides ( $CO_x$ ) contributing 3.04–4.35%, and carbon deposits contributing 1.04–1.54%. In summary, these product groups had a narrower range of contribution compared to olefins and aromatics.

The mass based yields (reported in parentheses in Table 6) obtained with the four bed materials can be compared with the results obtained by Jung and colleagues for fluidized bed conversion of HDPE at 728 °C, and Kaminsky's study on fluidized bed steam cracking of HDPE at 740 °C [2,20]. Silica-sand was used as the bed material in both studies. Methane, olefins, and mono aromatics were found to be the primary products in all cases. However, the product distributions obtained in this study were slightly different from those reported by Jung and Kaminsky. Kaminsky reported yields (wt%, feedstock) of 25.4%, 9.0%, and 3.1% for  $C_2$ ,  $C_3$ , and  $C_4$  olefins, respectively, whereas Jung et al. reported yields (wt%) of 21.5%, 10.5%, and 5.3% [2,20]. The combined yields of mono aromatics reported by Kaminsky and Jung et al. were 16.9 wt% and 14.5 wt%, respectively [2,20].

In addition to comparing the results obtained within this study, it is also valuable to assess the findings in relation to previous research conducted with different reactor configurations. Artexe et al. performed a two-step high-temperature thermal cracking process and achieved maximum yields of ethylene and propylene at 40.4 and 19.5 wt%, respectively, when operating the second step at 900 °C [8]. While the yields obtained in this study were slightly lower, they remain comparable to the results reported by Artexe et al. Another relevant study by Milne et al. employed an internally circulating fluidized bed reactor [7]. Their investigation yielded similar results at 780 °C to those obtained in this work, with ethylene and propylene yields reaching 28.2 and 17.8 wt%, respectively. These findings demonstrate that the yields of ethylene and propylene achieved in this study are consistent with those reported by Milne et al.

Finally, the "balance" characterizes the carbon content of unmeasured species in the reaction mixture. This group is determined by calculating the difference between the total carbon amount present in the feedstock, as listed in Table 3, and the carbon quantity measured in the resultant products. The unaccounted carbon is believed to correspond to aliphatic hydrocarbon species that contain more than four carbon atoms ( $C_5H_x$ ,  $C_6H_x$ , etc.). However, the analytical methods employed in this study were not capable of detecting such species. It is important to note that the assumption made regarding the identity of the unmeasured carbon is not definitive and should be validated through additional analytical techniques capable of detecting these larger hydrocarbon species.

#### 4.2. Hydrogen balance

Fig. 2 outlines the distribution of hydrogen atoms among different product groups obtained with olivine, bauxite, silica-sand, and feldspar as the bed materials. The product groups, namely  $H_2$ , Olefins, Aromatics, and Paraffins, account for a hydrogen balance closure of 91%, 87%,

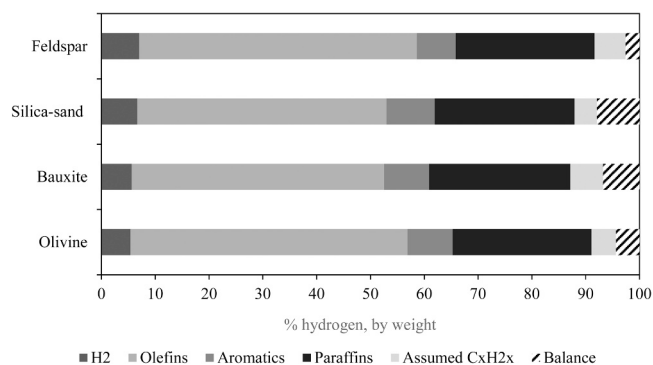


Fig. 2. Elemental hydrogen balance over the steam cracker.

88%, and 92%, for the four bed materials, respectively. The contribution of olefins to the hydrogen balance is calculated by grouping all  $C_3H_x$  and  $C_4H_x$  species as  $C_3H_6$  and  $C_4H_8$ , respectively. The unidentified hydrocarbon species mentioned in Table 6 contribute 5%, 6%, 4%, and 6% to the hydrogen balance for olivine, bauxite, silica-sand, and feldspar, assuming an empirical formula of  $C_xH_{2x}$ , which is the same as the polyethylene feedstock. Contributions based on the assumed identity of aliphatic hydrocarbons with three or more than three carbon atoms account for up to 20% of the total hydrogen balance for all four bed materials. The variations in these contributions will depend on the actual H/C ratio of  $C_3H_x$ ,  $C_4H_x$ , and heavier aliphatic hydrocarbons in the product mixture.

In Fig. 2, the group labeled as 'Balance' indicates the difference between the total amount of hydrogen in the feedstock and the calculated amount of hydrogen in the resulting products. The discrepancy in the hydrogen balance account for 4% with olivine, 7% with bauxite, 8% with silica-sand, and 3% with feldspar, due to the missing hydrogen atoms.

#### 4.3. Conversion

Fig. 3 presents the conversion rate obtained from the experiments, which are calculated according to Eq. 4, considering the overall yields of  $C_1 - C_4$  species, aromatics, PAHs, and carbon deposits.

The results show that all four bed materials were effective in converting the feedstock, with conversion rates ranging from 93.2% to 95.2%. Silica-sand demonstrated the highest conversion with a rate of 95.2%, while bauxite showed the lowest conversion with a rate of

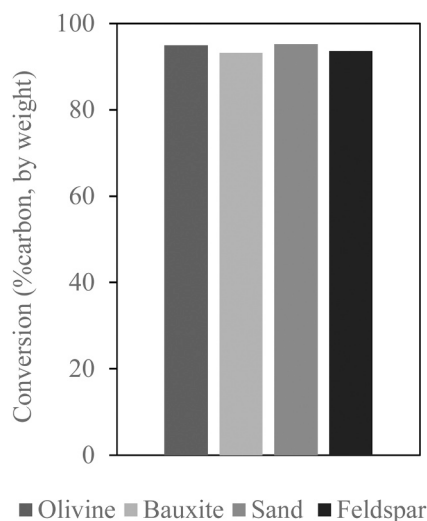


Fig. 3. Conversion rates obtained using olivine, bauxite, silica-sand and feldspar as bed materials.

93.2%. Olivine and Feldspar had conversion rates of 94.9% and 93.6%, respectively. The differences in conversion rates between the four bed materials were relatively small, with a maximum difference of only 1.3%.

#### 4.4. Cracking severity

The cracking severity coefficients for the four bed materials used in this study are presented in Fig. 4.

As mentioned earlier, the cracking severity coefficient is inversely proportional to the cracking severity of the process, meaning that lower values indicate a more severe cracking process. The cracking severity coefficient for olivine, bauxite, silica-sand, and feldspar, resulted in values of 2.13, 1.96, 1.93, and 2.13, respectively. It can be inferred that bauxite and silica-sand induced marginally higher levels of cracking severity when compared to olivine and feldspar.

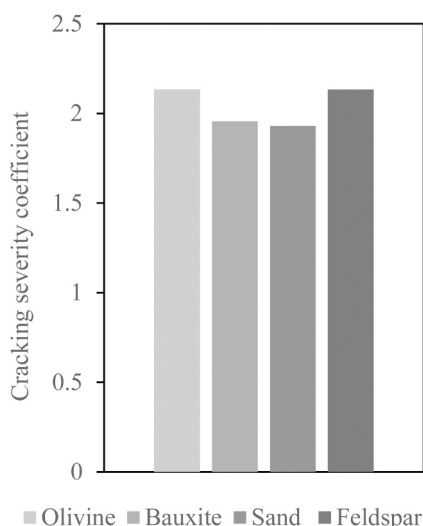


Fig. 4. Cracking severity coefficient obtained with the four bed materials.

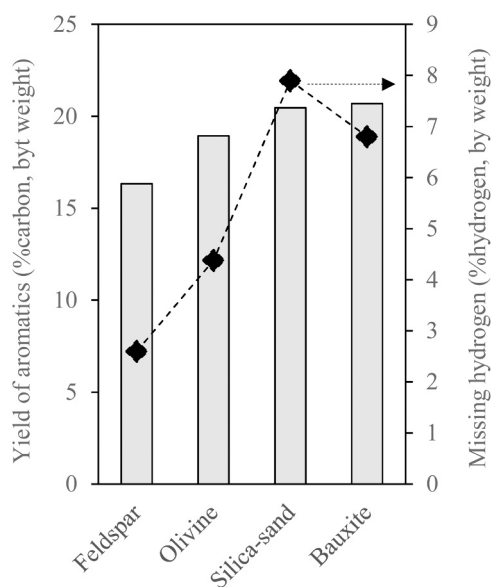


Fig. 5. Yield of aromatics and the amount of missing hydrogen. The missing hydrogen is the difference between the total hydrogen in the feedstock and the amount of hydrogen measured in the product mixture.

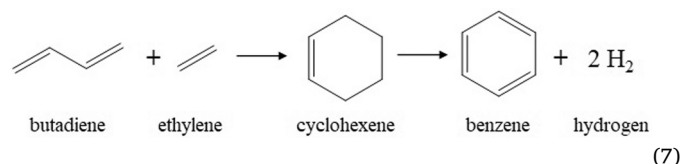
## 5. Discussion

The results indicate marginal differences in the performance of the fluidized bed steam cracker when operated with olivine, bauxite, silica-sand, and feldspar as bed materials, as indicated by the conversion and the cracking severity. In addition to the performance parameters, the yield of paraffins, carbon oxides, and solid carbon deposits also did not differ among the bed materials under the tested operating conditions.

Interestingly, variation in the product distribution among the bed materials was observed, particularly with respect to the yields of olefins and aromatics. Steam cracking in the presence of olivine and feldspar produced higher yields of olefins compared to silica-sand and bauxite. Conversely, the yields of aromatics were higher for silica-sand and bauxite compared to olivine and feldspar. These observations indicate that the bed materials have subtle but important differences in thermal or reactive interactions with the steam cracking process, which lead to the changes in cracking severity and product distribution. As discussed earlier, the variation in thermal interaction of the bed material could impact the cracking severity, while reactive interactions could interfere with the cracking reactions and influence the product distribution.

It is clear from the cracking severity coefficients (Fig. 4) that silica-sand and bauxite induced a higher cracking severity compared to olivine and feldspar. In the investigation of the impact of bed materials on cracking severity, it is crucial to consider the development of carbon deposits on the bed material surface during the cracking process. According to the literature on polyolefin cracking, the formation of carbon deposits, also known as coke, on the catalyst surface hinders the cracking reactions [21,22]. Table 6 reveals that the quantity of coke produced on the four bed materials had a narrow range of 0.89–1.32% by weight. Additionally, the combustion of the coke formed on the bed material surface during each batch of experiment (as indicated in Table 5) rendered the bed material free of coke prior to the next experiment batch. As a result, in this case, it is not possible to establish a correlation between coke formation and cracking severity.

Higher cracking severity typically results in a higher yield of aromatics, which is coupled with the secondary reactions of light olefins [15]. In the case of silica-sand and bauxite, the detrimental effect of the higher cracking severity on the light olefins can be explained by such secondary reactions. An example of a typical secondary reaction involved in hydrocarbon cracking is the Diels-Alder reaction of ethylene and butadiene [23], which is shown in Eq. 7.



The formation of aromatics, as shown in Eq. 7, is accompanied by the formation of molecular hydrogen in the product mixture. In addition, the hydrogen can also react with other species to form more stable hydrocarbons [24,25]. Therefore, it is expected that regardless of the cracking severity, the total amount of hydrogen (as  $\text{H}_2$  and hydrocarbons) in the product mixture should remain constant. Notably, under comparable operating conditions, silica-sand and bauxite yielded higher amounts of aromatics but lower hydrogen yields (as seen in Fig. 2) when compared to olivine and feldspar. Fig. 5 provides a visualization of the yield of aromatics and the yield of total hydrogen for the four bed materials.

The missing hydrogen in the product mixture of HDPE steam cracking may be attributed to the oxidation of the hydrogen atoms in the feedstock to  $\text{H}_2\text{O}$  by the bed material [12]. The results obtained in the present study indicate that both silica-sand and bauxite bed materials exhibited a higher amount of missing hydrogen compared to olivine and feldspar. This observation suggests that silica-sand and bauxite have a higher oxidizing nature than olivine and feldspar. The higher oxidizing



capability of silica-sand and bauxite can be attributed to their higher  $\text{Fe}_2\text{O}_3$  content, as shown in Table 2 [11]. Although olivine has a 70-fold higher level of  $\text{Fe}_2\text{O}_3$  than feldspar, its amount of missing hydrogen is much lower and is comparable to that of feldspar. This difference can be explained by the accessibility of iron in olivine. Olivine, being an iron-magnesium silicate, is known to have a low surface availability of iron oxide [26,27].

The preceding discussion reveals that, when used in their natural form, bed materials such as bauxite, olivine, and feldspar do not exhibit significant catalytic activity and produce product distributions comparable to that of silica-sand. This implies that the catalytic behavior reported in fluidized bed conversion literature for activated olivine, bauxite, and feldspar does not manifest in their natural state. The marginal differences observed in the yields of olefins and aromatics among the bed materials result from slight variations in their thermal and reactive interactions with the cracking reactions. Silica-sand and bauxite induce a slightly higher cracking severity and a more oxidizing environment in the steam cracker, which leads to higher yields of aromatics than olivine and feldspar. Furthermore, the increase in aromatics production observed with silica-sand and bauxite correlates to a higher level of reactive interaction of the bed materials during steam cracking, where H atoms are oxidized.

## 6. Conclusions

The study investigated the potential use of four different natural ores, including olivine, bauxite, feldspar, and silica-sand, as bed materials for steam cracking of polyethylene in a bubbling fluidized bed reactor at 750 °C. The performance of the steam cracker was measured in terms of cracking severity, conversion, and product distribution. Additionally, the impact of these bed materials on cracking reactions, including their thermal and reactive interactions, was investigated, and the findings were discussed in terms of their implications for catalytic activity.

The study found that there were only marginal differences in cracking severity among the different bed materials, and the conversion remained relatively consistent. The product distributions showed slight variation in the yields of light olefins and aromatics, while the yields of paraffins and carbon oxides were relatively constant. When comparing the yields of olefins and aromatics produced by olivine, feldspar, silica-sand, and bauxite, some interesting findings emerged. Olivine and feldspar showed higher olefin yields, whereas silica-sand and bauxite demonstrated higher aromatics yields. The slight differences observed in the product distribution and cracking severity indicate that, under the tested conditions, olivine, bauxite, silica-sand, and feldspar, in their natural forms, did not demonstrate a significant catalytic impact on the hydrocarbon cracking reactions.

## CRediT authorship contribution statement

**Chahat Mandviwala:** Conceptualization, Methodology, Investigation, Data curation, Writing-Original Draft. **Judith González-Arias:** Methodology & Investigation. **Teresa Berdugo Vilches:** Investigation, Writing-Review & Editing, Supervision. **Martin Seemann:** Conceptualization, Supervision, Writing-Review & Editing, Project administration. **Henrik Thunman:** Conceptualization, Writing-Review & Editing, Funding acquisition.

## Declaration of Competing Interest

The authors declare that they have no known competing financial interests or personal relationships that could have appeared to influence the work reported in this paper.

## Data Availability

No data was used for the research described in the article.

## Acknowledgments

This work was financially supported by Borealis AB, Sweden (Project number: 49514-1), the Swedish Gasification Center (SFC) and the Swedish Energy Agency. The authors thank Jessica Bohwalli, Johannes Öhlin and Rustan Hvitt for technical support during the experiments.

## References

- [1] H. Thunman, T. Berdugo Vilches, M. Seemann, J. Maric, I.C. Vela, S. Pissot, H.N. T. Nguyen, Circular use of plastics-transformation of existing petrochemical clusters into thermochemical recycling plants with 100% plastics recovery, *Sustain. Mater. Technol.* 22 (2019), <https://doi.org/10.1016/j.susmat.2019.e00124>.
- [2] W. Kaminsky, Chemical recycling of plastics by fluidized bed pyrolysis, *Fuel Commun.* 8 (2021), <https://doi.org/10.1016/j.fueco.2021.100023>.
- [3] M.S. Abbas-Abadi, Y. Ureel, A. Eschenbacher, F.H. Vermeire, R.J. Varghese, J. Oenema, G.D. Stefanidis, K.M. van Geem, Challenges and opportunities of light olefin production via thermal and catalytic pyrolysis of end-of-life polyolefins: towards full recyclability, *Prog. Energy Combust. Sci.* 96 (2023), <https://doi.org/10.1016/j.pecs.2022.101046>.
- [4] R. Geyer, J.R. Jambeck, K.L. Law, Production, use, and fate of all plastics ever made, *Sci. Adv.* 3 (2017), <https://doi.org/10.1126/sciadv.1700782>.
- [5] J. González-Arias, T. Berdugo-Vilches, C. Mandviwala, I. Cañete-Vela, M. Seemann, H. Thunman, Effect of biomass ash on preventing aromatization of olefinic cracking products in dual fluidized bed systems, *Fuel* 338 (2023), <https://doi.org/10.1016/j.fuel.2022.127256>.
- [6] Ullmann's Encyclopedia of Industrial Chemistry, Choice Rev. Online 50 (2012), <https://doi.org/10.5860/choice.50-1224>.
- [7] B.J. Milne, L.A. Behie, F. Berruti, Recycling of waste plastics by ultrapyrolysis using an internally circulating fluidized bed reactor, *J. Anal. Appl. Pyrolysis* 51 (1999) 157–166, [https://doi.org/10.1016/S0165-2370\(99\)00014-5](https://doi.org/10.1016/S0165-2370(99)00014-5).
- [8] M. Artetxe, G. Lopez, G. Elordi, M. Amutio, J. Bilbao, M. Olazar, Production of light olefins from polyethylene in a two-step process: pyrolysis in a conical spouted bed and downstream high-temperature thermal cracking, *Ind. Eng. Chem. Res.* 51 (2012), <https://doi.org/10.1021/ie300178e>.
- [9] Z. Fu, F. Hua, S. Yang, H. Wang, Y. Cheng, Evolution of light olefins during the pyrolysis of polyethylene in a two-stage process, *J. Anal. Appl. Pyrolysis* 169 (2023), <https://doi.org/10.1016/j.jaap.2023.105877>.
- [10] H.S. Cerqueira, G. Caeiro, L. Costa, F. Ramôa Ribeiro, Deactivation of FCC catalysts, *J. Mol. Catal. A Chem.* 292 (2008), <https://doi.org/10.1016/j.molcata.2008.06.014>.
- [11] T. Berdugo Vilches, J. Marinkovic, M. Seemann, H. Thunman, Comparing active bed materials in a dual fluidized bed biomass gasifier: olivine, bauxite, quartz-sand, and ilmenite, *Energy Fuels* 30 (2016), <https://doi.org/10.1021/acs.energyfuels.6b00327>.
- [12] C. Mandviwala, T. Berdugo Vilches, M. Seemann, R. Faust, H. Thunman, Thermochemical conversion of polyethylene in a fluidized bed: impact of transition metal-induced oxygen transport on product distribution, *J. Anal. Appl. Pyrolysis* 163 (2022), <https://doi.org/10.1016/j.jaap.2022.105476>.
- [13] C. Mandviwala, T. Vilches Berdugo, M. Seemann, J. González-Arias, H. Thunman, Unraveling the hydrocracking capabilities of fluidized bed systems operated with natural ores as bed materials, *J. Anal. Appl. Pyrolysis* 166 (2022), <https://doi.org/10.1016/j.jaap.2022.105603>.
- [14] A.M. Mauerhofer, F. Benedikt, J.C. Schmid, J. Fuchs, S. Müller, H. Hofbauer, Influence of different bed material mixtures on dual fluidized bed steam gasification, *Energy* 157 (2018), <https://doi.org/10.1016/j.energy.2018.05.158>.
- [15] Z. Gholami, F. Gholami, Z. Tisler, M. Vakili, A review on the production of light olefins using steam cracking of hydrocarbons, *Energ. (Basel)* 14 (2021), <https://doi.org/10.3390/en14238190>.
- [16] V. Wilk, H. Hofbauer, Conversion of mixed plastic wastes in a dual fluidized bed steam gasifier, *Fuel* 107 (2013), <https://doi.org/10.1016/j.fuel.2013.01.068>.
- [17] N. Berguerand, T. Berdugo Vilches, Alkali-Feldspar as a catalyst for biomass gasification in a 2-MW indirect gasifier, *Energy Fuels* 31 (2017), <https://doi.org/10.1021/acs.energyfuels.6b02312>.
- [18] W. Posch, Polyolefins, *Applied Plastics Engineering Handbook: Processing and Materials*, 2011, pp. 23–48, <https://doi.org/10.1016/B978-1-4377-3514-7.10003-0>.
- [19] M. Israelsson, M. Seemann, H. Thunman, Assessment of the solid-phase adsorption method for sampling biomass-derived tar in industrial environments, *Energy Fuels* 27 (2013), <https://doi.org/10.1021/ef401893j>.
- [20] S.H. Jung, M.H. Cho, B.S. Kang, J.S. Kim, Pyrolysis of a fraction of waste polypropylene and polyethylene for the recovery of BTX aromatics using a fluidized bed reactor, *Fuel Process. Technol.* 91 (2010), <https://doi.org/10.1016/j.fuproc.2009.10.009>.
- [21] E. Rodríguez, G. Elordi, J. Valecillos, S. Izaddoust, J. Bilbao, J.M. Arandes, P. Castaño, Coke deposition and product distribution in the co-cracking of waste polyolefin derived streams and vacuum gas oil under FCC unit conditions, *Fuel*

- Process. Technol. 192 (2019) 130–139, <https://doi.org/10.1016/J.FUPROC.2019.04.012>.
- [22] M. Ibáñez, M. Artetxe, G. Lopez, G. Elordi, J. Bilbao, M. Olazar, P. Castaño, Identification of the coke deposited on an HZSM-5 zeolite catalyst during the sequenced pyrolysis–cracking of HDPE, *Appl. Catal. B* 148–149 (2014) 436–445, <https://doi.org/10.1016/J.APCATB.2013.11.023>.
- [23] L. Dai, Y. Wang, Y. Liu, C. He, R. Ruan, Z. Yu, L. Jiang, Z. Zeng, Q. Wu, A review on selective production of value-added chemicals via catalytic pyrolysis of lignocellulosic biomass, *Sci. Total Environ.* 749 (2020), <https://doi.org/10.1016/j.scitotenv.2020.142386>.
- [24] G. Yan, X. Jing, H. Wen, S. Xiang, Thermal cracking of virgin and waste plastics of PP and LDPE in a semibatch reactor under atmospheric pressure, *Energy Fuels* 29 (2015), <https://doi.org/10.1021/ef502919f>.
- [25] M. Liu, J.K. Zhuo, S.J. Xiong, Q. Yao, Catalytic degradation of high-density polyethylene over a clay catalyst compared with other catalysts, *Energy Fuels* 28 (2014), <https://doi.org/10.1021/ef501326k>.
- [26] L. Devi, M. Craje, P. Thüne, K.J. Ptasinski, F.J.J.G. Janssen, Olivine as tar removal catalyst for biomass gasifiers: catalyst characterization, *Appl. Catal. A Gen.* 294 (2005), <https://doi.org/10.1016/j.apcata.2005.07.044>.
- [27] R. Faust, T. Berdugo Vilches, P. Malmberg, M. Seemann, P. Knutsson, Comparison of ash layer formation mechanisms on Si-containing bed material during dual fluidized bed gasification of woody biomass, *Energy Fuels* 34 (2020), <https://doi.org/10.1021/acs.energyfuels.0c00509>.